Response of Honeycomb Core Sandwich Panel with Minimum Gage GFRP Face-sheets to Compression Loading after Impact

Thomas D. McQuigg*[a], Rakesh K. Kapania[a], Stephen J. Scotti[b], Sandra P. Walker[b]
[a]Aerospace and Ocean Engineering, Virginia Polytechnic Institute and State University,
215 Randolph Hall, Blacksburg, VA, USA 24061;
[b]NASA Langley Research Center, Mail Stop 190, Hampton, VA USA 23681-2199

ABSTRACT

A compression after impact study has been conducted to determine the residual strength of three sandwich panel constructions with two types of thin glass fiber reinforced polymer face-sheets and two hexagonal honeycomb Nomex® core densities. Impact testing is conducted to first determine the characteristics of damage resulting from various impact energy levels. Two modes of failure are found during compression after impact tests with the density of the core precipitating the failure mode present for a given specimen. A finite element analysis is presented for prediction of the residual compressive strength of the impacted specimens. The analysis includes progressive damage modeling in the face-sheets. Preliminary analysis results were similar to the experimental results; however, a higher fidelity core material model is expected to improve the correlation.

Keywords: compression after impact, sandwich composite, finite element modeling, progressive damage modeling

1. INTRODUCTION

Understanding the effect of impact damage in composite aerospace structures is becoming increasingly important as use of composite materials for these structures is expanding rapidly. Composite materials, which are used in a variety of critical load bearing components, are also susceptible to impact damage during manufacture and service. Low speed impact damage has been reported to cause catastrophic loss of structural integrity in composites, even when damage was not visibly evident [1-9, 18]. Design efficiency often suffers because of the complexity and lack of understanding associated with this damage.

The focus of the present effort is the response and residual strength of impact damaged honeycomb core sandwich structures having thin, glass fiber/epoxy composite face-sheets subjected to uniaxial compressive loading. An investigation of impact damaged composite load bearing components through experiments is described. Preliminary results of a finite element analysis for predicting the residual strength of similar panels using Abaqus® (Dessault Systems) software combined with a progressive failure analysis using Helius:MCT^{TM} (Firehole Technologies, Inc.) are presented.

2. BACKGROUND REVIEW

2.1 Compression after Impact

Attempts to understand impact damage will have one of the two following foci: either damage resistance, the study of a material's ability to withstand impact without sustaining damage, or damage tolerance, the study of a material's ability to carry design loads while damaged. Both factors are necessary to characterize a given material. The purpose of the present research was to understand the damage tolerance of thin face-sheet honeycomb core sandwich panels, although their resistance to impact was also evaluated to a small degree. To this aim, compression after impact (CAI) of small sandwich coupons was studied to measure the reduction of material integrity with a given impact damage.

*tmcquigg@vt.edu; phone 1 757 864-2531; www.aoe.vt.edu

Although shear and tension after impact can also be used to characterize material response to damage, CAI often demonstrates a more drastic reduction in material strength due to the shear strength driven interply delaminations encountered from the compressive load, which often present in impact damaged laminates. The characteristics of CAI failure was shown by Rhodes, Williams, and Starnes [1] for thick laminates as well as by Elber [2] for thin composite plates. Rhodes also studied impact and CAI failure in composite sandwich panels [3, 4], as have Ambur and Cruz [5], and Tsang and Lagace [6]. These works show that impact damage and resulting CAI failure is a critical phenomenon in sandwich structures. The structural response and failure characteristics of laminated composite structures have been evaluated experimentally for many composite panel geometries, such as Starnes *et al* study of plates [7] and Rhodes *et* al investigation of hat-stiffened panels [8]. An example of multi-rib and multi-spar component level test is described by Demuts *et al* [9]. Tomblin *et al* has presented damage resistance and tolerance studies using CAI testing on honeycomb core sandwich panels [10].

2.2 Modeling and Analysis

To safely use composites in impact damage susceptible components, designers impose high safety margins or strength "knock downs" to account for drastic reductions of strength due to damage observed in experimental data. Since experimentally determining the damage tolerance of every component designed is neither resourceful nor cost effective, modeling and analysis to predict failure have become an increasingly important focus of CAI studies. Several authors have described design techniques that rely heavily on CAI test data to predict failure. A progressive failure methodology was investigated by Schubel *et al.* [11]. A similar methodology to develop a material strength design value was used by Nettles and Jackson [12]. This type of prediction still requires expensive and time-consuming experimental testing. Although all models and analysis require experimental validation, alternative methods can limit this cost to the design process.

Closed-form analytic solutions have been used by several authors. Staal, Mallinson, and Jayaraman presented a solution based on the buckling characteristics of a thin, indented plate on an elastic foundation [13]. An earlier analytic solution using a single parameter model with experimental validation was put forth by Kassapoglou and Abbot [14]. In Ref. 14, the authors assume that delamination is the predominant damage produced by the impact and driver of a compression load related failure. However, their methodology ignores the effect of a residual dent which can have a significant effect on damage progression and ultimate failure in thin face-sheet sandwich panels.

An analytic solution was used by Minguet to predict the effect of the residual dent and associated core and face-sheet damage on compressive load tolerance [15]. Minguet's model has proved to be complex in implementation and computationally intensive. The fidelity of subsequent analytic models has been reduced for computational efficiency. Tsang offered one revised model that included an elastic foundation core, described by two parameters used as a fit for the displacement and stress distribution [16]. Xie and Vizzini offered a further revised model with a simple one-parameter model [17]. Often analytic models, especially when they are simple, incorporate many assumptions to arrive at a closed form solution.

Other researchers have turned to finite element modeling (FEM) as a means of including more realistic damage (e.g. core crushing) while still limiting implementation complexity and computational time. Ratcliffe and Jackson have expanded on the work and input of Minguet, Tsang, and Xie through a simple FEM which includes a single shell represented face-sheet and a non-linear spring element model for the elastic support provided by the core [18]. McQuigg *et al* used this model with minor modification and were able to accurately make predictions for some of the experimental results presented [19]. Another group of researchers made use of the implementation efficiency of modern commercially available finite element analysis (FEA) software to create a much higher fidelity FEM. Czabaj *et al* included hexagonal honeycomb geometry in their core model and also modeled the indentation of the core model itself to provide enhanced fidelity [20].

The present research includes an implementation of progressive damage modeling in the face-sheets. The implementation of progressive damage modeling is an active research area. One implementation which uses the well-known Hashin failure initiation model was implemented by Lapczyk and Hurtado [21] in Abaqus FEM. Attempts to account for the effects of micro-mechanics have led to the use of multi-continuum theories, such as the work by Mayes and Hansen. [22]. The work by Mayes *et al* was implemented by Firehole Technologies, Inc. in their software Helius:MCT, which is utilized in this work.

3. DESCRIPTION OF EXPERIMENTS

3.1 Materials and Test Coupons

Several test methods were considered when the CAI tests described in this section were designed. ASTM standard test methods (STM) were consulted, but a STM for compressive residual strength of sandwich constructions has not currently been adopted. The STM for compressive residual strength of composite plates does describe a procedure and special test fixture for simple plates with centrally located impact damage [23]. This STM was consulted for strain gage placement and allowable failure modes. The STM for edge-wise compressive strength (undamaged) of sandwich constructions was also considered [24]. This test method was consulted for sizing of the damaged panels, since the increased bending stiffness of sandwich constructions should preclude the use of the test fixture described in Ref. 23.

CAI test coupons were fabricated from three sets of honeycomb core sandwich panels with minimum gage face-sheets. The first set of material coupons was designated P01 through P12 although only 10 coupons were tested in compression and will be referred in general in this document as PXX series materials. These materials were manufactured by AAR Composites and consisted of glass fiber reinforced polymer (GFRP) face-sheets and Nomex® hexagonal honeycomb core. Each face-sheet of the sandwich construction consisted of two plies of style 7781 plain woven E-glass fabric with 40% epoxy resin content. The plies were directionally aligned in the 0° direction and the nominal cured thickness for a single face-sheet was 0.020 in. The honeycomb core was 1 in. thick with 0.125 in. cell size and had a density of 3.0 lb/ft.^{3}. The PXX material is shown in Fig. 1, where the translucent property of the thin GFRP face-sheets allows for viewing of the core underneath. This property also allows for improved visual inspection for damage and manufacturing imperfection that may be present in the material.

Figure 1. PXX sandwich panel material (left) and PXX material coupons (right).

Test coupons were prepared from PXX material at the nominal size of 6 in. by 6 in. The test coupons are shown in Fig. 1.These coupons were used in all of the tests described in the next section. To avoid premature coupon failure for the uniaxial compression tests, special considerations for load introduction were made. At the top and bottom (the load bearing ends of each coupon) a section of core material was removed from between the face-sheets. This section had dimensions of the width (6 in.) and thickness (1 in.) of the coupon and it extended in the loading direction approximately 0.5 in. A clay “potting” material was used to fill this void. The purpose of this was to increase the surface area for load transfer between the compression test frame and the coupon. In addition, the potting limited the out of plane bending (or “brooming”) of the coupon face-sheets’ load direction edges, due to the applied compression load. The potting on the ends of each coupon was ground to straight and level to a tolerance of 0.001 in.

The second and third sets of sandwich panel materials were similar in construction. Two hexagonal honeycomb core materials with different densities were used; therefore, their coupons’ series names, 3PCF-XX and 6PCF-XX (where XX refers to the individual coupon number), refer to core densities of 3 lb./ft.^{3} and 6 lb./ft.^{3}, respectively. These two sandwich panel constructions will be referred to in this document as 3PCF and 6PCF for short. The other material properties for these sandwich constructions are as follows. The core material remains Nomex® and the cell size remains 0.125 in. The thickness of the core is 0.75 in. The face-sheets consist of two plies of style 6781 S2-glass fabric with 35% epoxy resin content. The two plies were oriented with ply directions of 0° and 45°, and the nominal face-sheet thickness was again 0.02 in.

Figure 2. Comparison of wood filled (top) and potting material filled (bottom) coupon ends.

Coupon attributes of the 3PCF and 6PCF sandwich constructions were changed slightly based on source material limitations and lessons learned from potting of the PXX material. The coupon size was still nominally 6 in. by 6 in. but the actual dimensions of each coupon are slightly smaller due to the size of the received source material panels. The potting approach was slightly different as well. It was found that the potting clay used in the PXX test series shrunk when cured which introduced bending stresses in the face-sheets. A study was conducted to evaluate two alternative approaches. A clay potting material having less contraction during cure was considered. In addition, a block of wood inserted with close clearances between the face-sheets and fastened with an epoxy resin was examined. A comparison of samples using the two approaches is shown in Fig. 2. It was determined that the wooden insert could be specifically sized to allow little or no introduction of out of plane displacement of the face-sheet edges; this method was thus used in the 3PCF and 6PCF compression coupons shown in Fig. 3.

Figure 3. 6PCF (left) and 3PCF material coupons.

3.2 Impact Damage Evaluation

A set of preliminary experimental tests was run on each sandwich panel construction to determine a range of impact energies which would range from damage threshold to clearly visible damage. First static indentation of each sandwich construction was done to determine rough bounds on the impact energies of interest. The static indentation apparatus and test fixture is shown in Fig. 4. A test coupon was clamped on all four edges using a special test fixture and then indented in a controlled quasi-static fashion using a 0.5 in. diameter hemispherical indentation tip. Force and displacement data was recorded during each test. An example of the resulting data is shown in Fig. 4. The total energy, represented by the area under the curve, was calculated to be 1.39 ft-lbs. The force vs. displacement response is mostly linear until face-sheet failure which is marked by a sudden drop in reaction force as displacement continues to increase. In Fig. 4, this occurs at about 0.1 inches of displacement. The energy absorbed by the panel to this point is 0.52 ft-lbs. It can also be noted that the initial slope of the linear portion of this curve is higher for the first 20 lbs. of force. This reduction in slope was found to be related to the initial buckling of the honeycomb core cell walls by observation. Static indentation is known to be a conservative estimate of the impact energy required for similar damage during a drop impact of the same type of indentation tip. Thus it is only a rough estimate of the energies of interest for a drop impact survey.

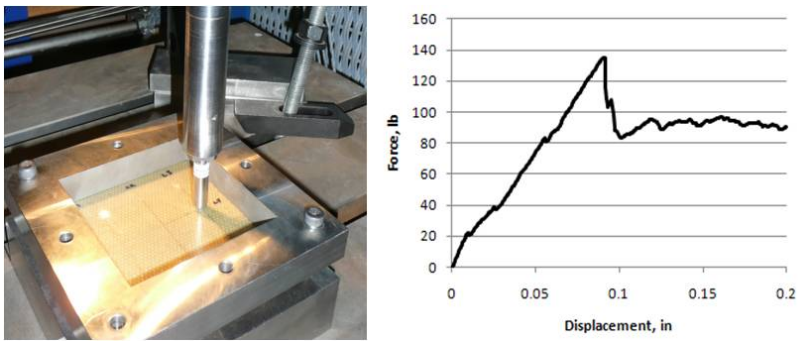

Figure 4. Static indentation testing (left) and sample force vs. displacement results (right).

The drop impact survey was the second of two preliminary tests run to determine the impact energy levels of interest for CAI testing. The purpose of the impact survey was to determine the characteristic damage at various impact energy levels. A material coupon was clamped on all four edges in a special test fixture with no support under the opposite face-sheet; this boundary condition is considered to be characteristic of a real world structural impact. The test fixture was then mounted to a robust steel table using heavy bolts. A 0.5 in. diameter hemispherical tipped impactor was measured to determine its mass. The drop height for a given impact energy level could then be calculated. During an impact event, reaction force vs. time information was recorded. The impact survey test fixture and apparatus is shown in Fig. 5 with example force vs. time results for a 5 ft-lb. impact energy level. At this energy level, the impact resulted in considerable face-sheet cracking, which absorbs substantial energy. Note the sudden drop in force at 0.01 sec. and the subsequent rapidly oscillating force level prior to tailing off.

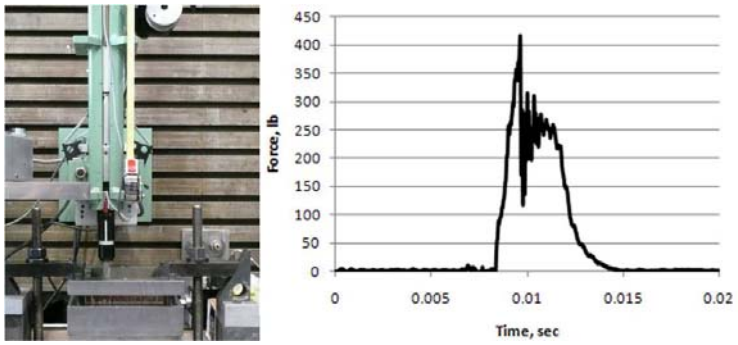

Figure 5. Impact survey test fixture and apparatus (left) and sample results for a 5 ft-lb. impact (right).

Once the impact survey was complete, each residual dent that resulted from a given impact was measured to determine its diameter and maximum depth as a general characterization of the damage. In addition, measured and visual qualitative observations were made about the location and characteristics of other types of damage present, including cracking or penetration of the impacted face-sheet. A few panels were also carefully dissected at the midpoint of the residual dent. Observations were then made to determine the extent and level of core damage that resulted from each impact. In addition, measurements could be accurately made to determine the profile of the core damage and the residual dent in the face-sheets. Example images of the interior of dissected impact dents are shown in Fig. 6.

Once all of this information was collated, a decision was made about which damage levels would be the most interesting for CAI testing. For the PXX sandwich materials, impacts were studied at energy levels from 0.5 to 2.5 ft-lbs. at 0.5 ft-lb. increments. Energy levels of 0.5, 1.0, 1.5 and 2.0 ft-lb. were chosen for impacting CAI coupons of these sandwich panels. Impacts on 3PCF and 6PCF series sandwich materials were studied from 1 ft-lb. to 9 ft-lb. at 1 ft-lb. increments. Energy levels of 1.0, 3.0, 5.0, and 7.0 ft-lb. were chosen for impacting coupons for CAI testing of these sandwich panels.

Figure 6. Examples of interior damage images at 1.0 (left), 3.0 (center), and 5.0 (right) ft-lbs. for 6PCF type sandwich panel construction.

3.3 Compression after Impact Tests

A servo-hydraulically actuated MTS load frame with a 100-kip maximum load was used for the CAI tests. The sandwich panel coupons were clamped at the top and bottom and mounted between two square loading platens. Loading was displacement controlled and applied through the upper platen at a rate of 0.02 in. per minute for the PXX sandwich constructions and at a rate of 0.01 in. per minute for the 3PCF and 6PCF sandwich constructions. Coupon alignment was adjustable through the lower platen as well as a smaller circular platform placed in between the lower coupon clamp and the lower platen. The CAI apparatus is shown in Fig. 7.

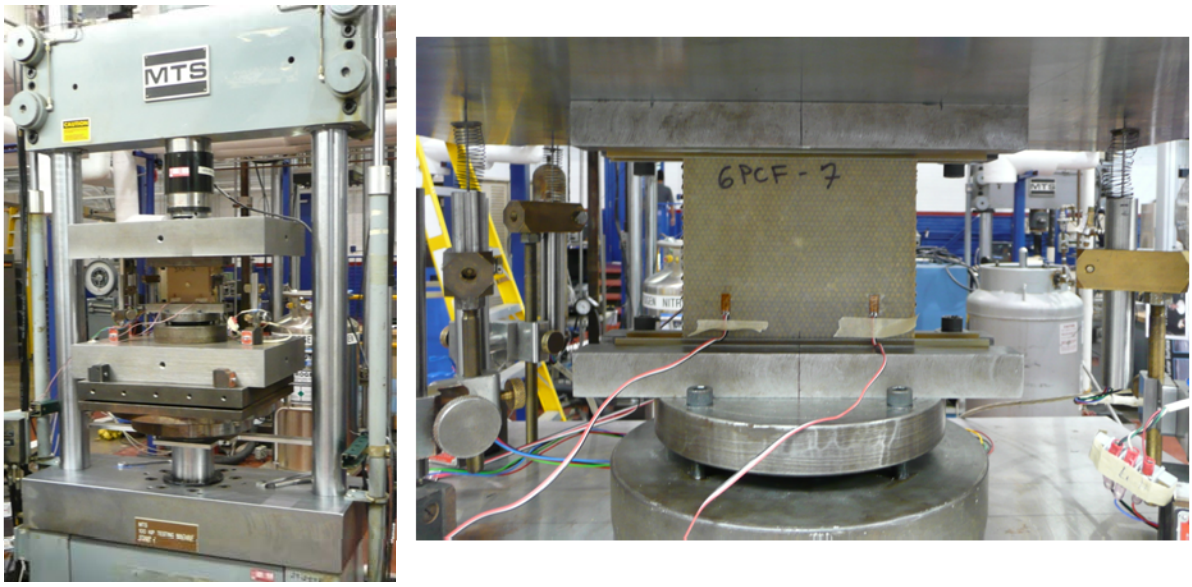

Figure 7. Compression after impact test apparatus.

For each CAI, test the applied displacement and the measured reaction force were recorded. Instrumentation included at least three, and up to five, strain gages placed as described in Ref. 23 with an additional strain gage placed centrally on the coupon, but on the rear, undamaged face-sheet. Also, three direct current displacement transducers (DCDT) were mounted to monitor the displacement at several locations between the loading platens. Two were located along the centerline of the coupon in the width direction at a distance of eight inches from the coupon's midpoint. The third DCDT was mounted at the same distance from the coupon to one side but at four inches from the centerline. These three instruments could then be used as auxiliary instrumentation to monitor any applied bending. In addition, for the CAI tests of the 3PCF and 6PCF constructions, a fourth DCDT directly monitored the out of plane displacement of the center of the sandwich coupon. Additional instrumentation used for observation of selected tests included video recording, high speed photography, and three dimensional digital image correlation for displacement and strain measurement on the surface of the damaged face-sheet.

4. CAI EXPERIMENTAL RESULTS AND DISCUSSION

4.1 CAI Tests of PXX Sandwich Constructions

Coupons of PXX sandwich construction materials were tested with a centrally located impact of energy level 0.5, 1.0, 1.5, or 2.0 ft-lb. Two panels were tested at each damage level and two additional panels were tested without impact damage for reference. The typical force vs. displacement response for a CAI test is shown in Fig. 8. The force-displacement behavior is linear until panel failure is observed, at which time there is then a sudden drop in the reaction force. Nominal failure stress and average far-field failure strain were reported for each test case and the results are shown in Fig. 9.

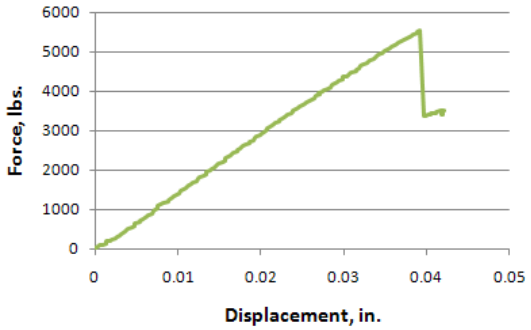

Figure 8. Typical force vs. displacement results for CAI tests.

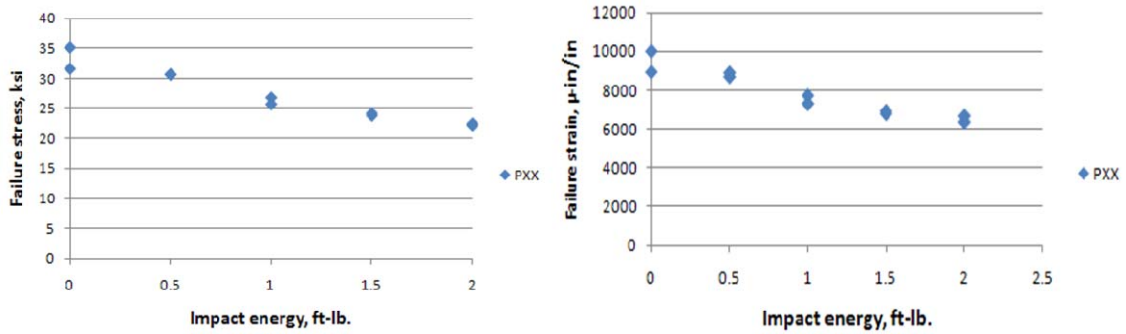

Figure 9. Failure stress (left) and strain (right) vs. impact energy for CAI tests of PXX sandwich constructions.

4.2 CAI Tests of 3PCF and 6PCF Sandwich Constructions

Impact damage was applied to 3PCF and 6PCF sandwich construction coupons at 1.0, 3.0, 5.0, and 7.0 ft-lb. impact energy levels. Three coupons were tested at each of the impact energy levels for each of the two types of sandwich constructions. Failure stress and strain are reported for each test case in Fig. 10 as well as one undamaged 3PCF panel for reference. Since the face-sheet construction is identical for 3PCF and 6PCF constructions, this undamaged data point is also assumed to be the ultimate strength of an undamaged 6PCF coupon.

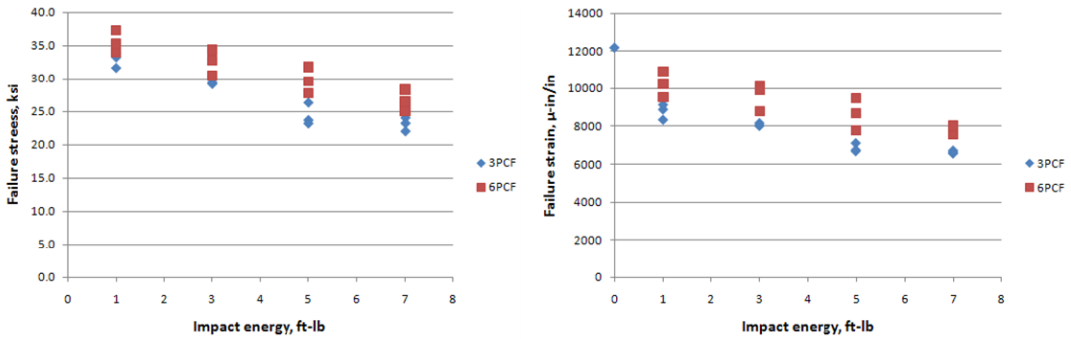

Figure 10. Failure stress (left) and strain (right) vs. impact energy for CAI tests of 3PCF and 6PCF sandwich structures.

4.3 Discussion of CAI Results

Several results are noteworthy from the CAI failure results presented in the previous two sections. Importantly, impact damage resulted in severe ultimate strength reductions, even for very low impact energy levels. The S2-glass face-sheet coupons (3/6PCF) had, as expected, higher strength then E-glass specimens. A CAI strength plateau is often noted in literature where the residual strength approaches a constant with increasing impact energy. For PXX sandwich constructions, the data seems to be approaching a constant already when impacted by the 2 ft-lb impact energy level as determined by the similar residual strengths of 1.5 and 2.0 ft-lb impact energy levels. This constant appears to be around 6000 micro-strain. For S2-glass face-sheet construction 3PCF, the same leveling off that appears around the 6000 micro-strain level, but does so at a far higher impact energy level, highlighting thus the damage tolerance superiority of S2 glass. In addition, the higher density core further increases the CAI strength almost to the 8000 micro-strain level for the same impact energies.

Another interesting result of these CAI tests was that two different failure modes were obtained. The PXX and 3PCF series constructions exhibited similar failure mode, while the increased core density of the 6PCF series construction excited a different failure mode. A visual comparison of post-failure specimens can be seen in Fig. 11, although the differences between the two failure modes are not completely highlighted. Video recording, and especially high-speed photography were instrumental in determining the characteristics of each failure mode. Combined with FEM analysis, this is being further examined. Essentially, the lower density core coupons exhibit a “dimple propagation” failure mechanism seen in literature [14-17]. In this case, the initial residual dent propagates transverse to the applied load in a stable manner until the failure load is reached at which point the damaged face-sheet catastrophically buckles. The higher density core maintains local stability of the face-sheet. Instead, of dimple propagation, both the face-sheet material strength and the delamination behavior tend to control failure.

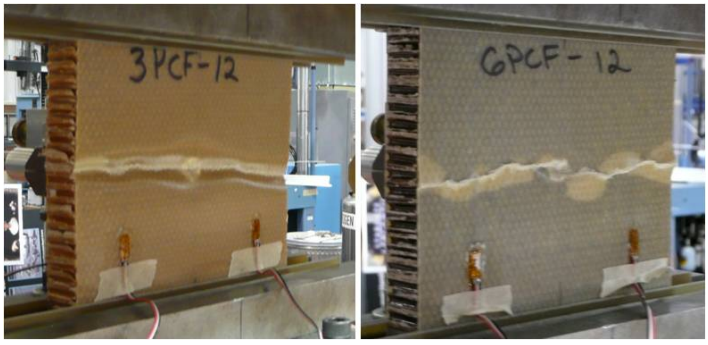

Figure 11. Comparison of failure modes, 3PCF (left) and 6PCF (right) honeycomb cores, both with 5 ft-lb impacts prior to CAI test.

5. FINITE ELEMENT ANALYSIS

5.1 Finite Element Model

A finite element model has been constructed to examine CAI failure in thin face-sheet honeycomb core sandwich panels with impact damage. The CAI coupons described in section 3 have been modeled using Abaqus/CAE [25]. Currently, an entire coupon is modeled including front and rear face-sheets and core. Core and face-sheet damage has been included in the model as a reduction to the constitutive coefficients in regions with location and size determined from experimental evidence. The core has been modeled as an orthotropic solid with three-dimensional solid elements. The face-sheets have been modeled using continuum shell elements which discretize each ply in the laminate. Helius:MCT software has been used to conduct a progressive damage analysis of the face-sheets [26]. Pinned boundary conditions are used at the top and bottom surfaces of the sandwich panel and load is displacement controlled from the top surface.

5.2 Preliminary FEM Results

A single test condition has been modeled with included damage to simulate the result of a 5 ft-lb. impact at the center of the sandwich panel coupon with S2-glass face-sheets and 3 lb/ft.^{3} Nomex® honeycomb core construction (i.e. 3PCF sandwich construction as described earlier). From the experimental results, a 3PCF construction with this type of

damage failed between 5100 and 5700 lbs. as determined from the force vs. displacement data available. For the current FEM, global failure is predicted at 6600 lbs., while Helius:MCT calculates local matrix failure beginning at a much lower value and local fiber failure beginning shortly before global failure. Some out of plane displacement is present but not as much as expected from experimental results. A core damage propagation model is currently being added that should reduce the stress and strain levels for predicted global failure and make the model more accurate qualitatively and quantitatively. Example results for output variables of out-of-plane displacement and fiber and matrix failure are shown in Fig. 12. Out of plane displacement is similar to experimental results when compared to Fig. 11 (left), but the amount of displacement is smaller and concluded to be due to the lack of a core crushing model. Out of plane displacement increases in the negative out of plate direction (into the panel) as the color changes from red to green. Local constituent failures predicting by Helius:MCT are also shown. Fiber (with matrix) failure is shown in red and matrix failure is shown in green. The analysis results are similar to the experimental test.

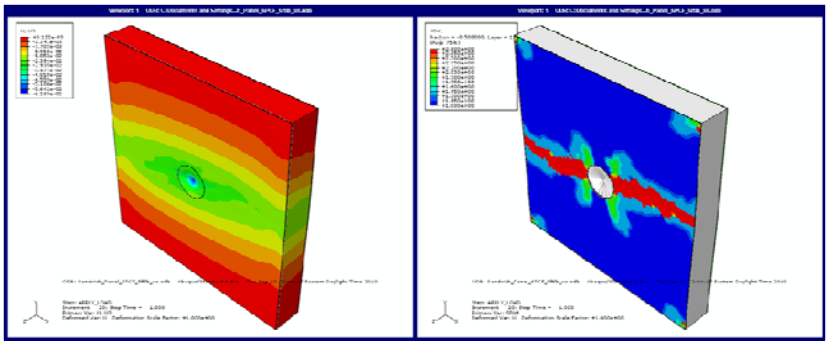

Figure 12. Example out of plane displacment and local constituent failure from FEM results.

6. CONCLUSIONS

Compression after impact testing is an important measure of a composite material's damage tolerance. Its use in this capacity was presented for a variety of sandwich constructions with GFRP face-sheets. With the ever increasing use of composites in aerospace structure for their high stiffness and strength to weight ratio, and especially sandwich panels for their high bending stiffness and low mass, the importance of an understanding of the effect of damage on these structures is well known. A brief summary of efforts to model this type of behavior has highlighted a large range of methods with varying assumptions and complexities.

Experimental results for compression after impact testing of three honeycomb core sandwich panels with thin-gage GFRP face-sheets was presented. Significant reductions in strength were obtained, even for small impact energies. Two different failure modes were found as a result of these experiments. Currently a FEM is being developed that includes progressive damage analysis capability to predict CAI failure of sandwich constructions. To accurately predict the experimental results, where failure mode depends on the core properties of the sandwich construction, a higher fidelity core model is currently being incorporated in the FEM.

REFERENCES

[1] Rhodes, M.D., Williams, J.G., and Starnes, Jr., J.H. "Low velocity impact damage in graphite-fiber reinforced epoxy laminates." 34th Conf. of the Reinforced Plastics/Composites Institute. Jan. 29 – Feb. 2, 1979.

[2] Elber, W. "Failure mechanics in low-velocity impacts on thin composite plates." NASA Technical Paper 2152. May 1983.

[3] Rhodes, M.D. "Low velocity impact on composite sandwich structures." 2nd Air Force Conference on Fibrous Composites in Flight Vehicle Design. May 1974.

[4] Rhodes, M.D. "Impact fracture of composite sandwich structures." AIAA/ASME/SAE 16th Structures, Structural Dynamics and Materials Conf. May 1975.

[5] Ambur, D.R. and Cruz, J. "Low speed impact response characteristics of composite sandwich panels." AIAA-95-1460. 1995.

[6] Tsang, P.H.W. and Lagace, P. "Failure mechanisms of impact-damaged sandwich panels under compression." 35th AIAA/ASME/ASCE/AHS/ASC Structures, Structural Dynamics and Materials Conference. 1994.
[7] Starnes, Jr., J.H., Rhodes, M.D., and Williams, J.G. "Effect of impact damage and holes on the compressive strength of a graphite/epoxy laminate." ASTM Special Technical Publication 696. 1979.
[8] Rhodes, M.D., Williams, J.G. and Starnes, Jr., J.H. "Effect of low-velocity impact damage on the compressive strength of graphite-epoxy hat-stiffened panel." NASA TN D-8411. April 1977.
[9] Demuts, E., Whitehead, R.S., and Deo, R.B. "Assessment of damage tolerance in composites." International Conference on Structural Impact and Crashworthiness, Imperial College, London, UK. July 1984.
[10] Tomblin, J.S., Raju, K.S., Liew, J. and Smith, B.L. "Impact damage characterization and damage tolerance of composite sandwich airframe structures." DOT/FAA/AR-00/44. January 2001.
[11] Schubel, P.M., Rome, J.I., Goyal, V.K., Tuck-Lee, J.P., "Predicting failure of damaged composite sandwich structures using compression-after-impact strength data." 50th AIAA/ASME/ASCE/AHS/ASC Structures, Structural Dynamics, and Materials Conference, 2009.
[12] Nettles, A.T., and Jackson, J.R. "Developing a material strength design value based on compression after impact damage for the Ares I composite interstage." NASA/TP-2009-215634. 2009.
[13] Staal, R.A., Mallinson, G.D., Jayaraman, K., and Horrigan, D.P.W. "Predicting failure loads of impact damaged honeycomb sandwich panels." Journal of Sandwich Structures and Materials. Vol. 11. March-May 2009.
[14] Kassapoglou, C. and Abbot, R. "A correlation parameter for predicting the compressive strength of composite sandwich panels after low speed impact." 29th AIAA/ASME/ASCE/AHS/ASC Structures, Structural Dynamics, and Materials Conf. April 1988.
[15] Minguet, P.J. "A model for predicting the behavior of impact-damaged minimum gage sandwich panels under compression." AIAA/ASME/ASCE/AHS/ASC 32nd Structures, Structural Dynamics and Materials Conf.AIAA-91-1075. 1991.
[16] Tsang, P.H.W. "Impact resistance and damage tolerance of composite sandwich panels." Ph.D. dissertation, Massachusetts Institute of Technology, 1994.
[17] Xie Z., and Vizzini, A.J. "Damage propagation in a composite sandwich panel subjected to increasing uniaxial compression after low-velocity impact." Journal of Sandwich Structures and Materials." Vol. 7. 2005.
[18] Ratcliffe, J.G. and Jackson, W.C. "A finite element analysis for predicting the residual compressive strength of impact-damaged sandwich panels." NASA/TM-2008-215341. 2008.
[19] McQuigg, T.D., Kapania, R.K., Scotti, S.J., and Walker, S.P. "Compression after impact testing of thin-facesheet honeycomb core sandwich panels." 18th International Conference on Composites and Nano Engineering. July 2010.
[20] Czabaj, M.W., Zehnder, A.T., Davidson, B.D., Singh, A.K., and Eisenberg, D.P. "Compression after impact of sandwich composite structures: experiments and modeling." 51st AIAA/ASME/ASCE/AHS/ASC Structures, Stuctural Dynamics, and Materials Conference. 2010.
[21] Lapczyk, I., and Hurtado, J.A. "Progressive damage modeling in fiber-reinforced materials." Composites, Part A: Applied Science and Manufacturing. January 2007.
[22] Mayes, J.S., and Hansen, A.C. "Composite laminate failure analysis using multicontinuum theory." Composites Science and Technology. Vol. 64. 2004.
[23] ASTM Standard D 7137/D 7137M – 07. "Standard test method for compressive residual strength properties of damaged polymer matrix composite plates." Dec. 2007.
[24] ASTM Standard C 364/C 364M – 07. "Standard test method for edgewise compressive strength of sandwich constructions." April 2007.
[25] Abaqus®/Standard Version 6.9-1. Dessault Systems. 2009.
[26] Helius:MCT™ Version 3.1. Firehole Technologies, Inc. 2009.